J Mater Sci (2010) 45:2633–2639
DOI 10.1007/s10853-010-4241-x

# Rubber-toughened epoxy loaded with carbon nanotubes: structure–property relationships

**Maria d. M. Salinas-Ruiz · Alex A. Skordos · Ivana K. Partridge**

Received: 28 October 2009 / Accepted: 13 January 2010 / Published online: 29 January 2010


**Abstract** The paper reports on the preparation, structure and properties of ternary thermosetting blends, based on DGEBA epoxy, cured with 3,3′-DDS and modified by the addition of CTBN reactive liquid rubber and/or 0.3 wt% of commercial multi-walled carbon nanotubes. The toughening effect of the phase-separated rubber particles is enhanced by the presence of the nanotubes, through a change in the morphology. In the absence of the rubber, the nanotubes alone produce a minimal effect upon the thermo-mechanical characteristics of the resin. However, the electrical conductivity of the cured resin samples is found to increase by five orders of magnitude, up to $3.6 \times 10^{-3}$ S/m in the ternary blend.

## Background

This paper reports a fundamental study of hitherto little studied ternary epoxy-based blends, containing a commercial rubbery modifier and commercial carbon nanotubes. The context of the original study was the identification of possible means to minimise the thermal residual stresses usually created in the manufacture of adhesively bonded aluminium-to-composite joints, such as structural elements of current aerospace structures. A model adhesive was formulated for 120 °C cure, with the intention of identifying the critical parameters in terms of processability and performance, in pursuit of the aim. Commercial multi-walled carbon nanotubes were included in the adhesive as they were believed to be capable of reducing the coefficient of thermal expansion of the resin [1, 2]. The accompanying expected increase in the thermal and electrical conductivity was considered to be of secondary importance to the intended application. A commercial rubbery adduct was used to toughen the resin [3, 4] to the level expected in relevant commercial adhesive systems. This paper focuses on the description of the microstructures of the cured resin blends and their thermo-mechanical, mechanical and electrical properties in the solid state.

M. d. M. Salinas-Ruiz (✉) · A. A. Skordos · I. K. Partridge
Department of Materials, Cranfield University, Composites Centre, Bedfordshire MK43 0AL, UK
e-mail: M.Salinas-Ruiz@bristol.ac.uk

## Material composition, preparation and thermo-analytical characterisation

The epoxy resin was a standard diglycidyl ether of bisphenol-A (DGEBA), (Araldite MY750, Huntsman; 182 g/eq epoxide equivalent weight), cured with 34 wt% of a solid aromatic diamine, 3,3′-diamino diphenyl sulphone (3,3′-DDS, Aldrich) and accelerated with 1 wt% boron trifluoride–monoethylamine ($BF_3$–MEA, Chemos GmbH). The rubber was a carboxyl-terminated butadiene-acrylonitrile (CTBN) rubber (Hypro CTBN 1300x8, Emerald Performance Materials; 18% acrylonitrile content) which has been pre-reacted with DGEBA resin to give a 40 wt% CTBN-epoxy adduct, (HyPox RA840, Emerald Performance Materials; 340 g/eq epoxide equivalent weight) (Fig. 1). The adduct was employed to lead to a concentration of 5 wt% CTBN rubber in the final product. In the formulations containing the rubber adduct the amount of DDS was reduced so as to maintain the chemical stoichiometry of the base resin matrix.

The multi-walled carbon nanotubes (MWCNTs) (NC-7000, Nanocyl) were added to the epoxy resin to achieve a concentration of 0.3 wt% in the final composite.

**Fig. 1** CTBN-epoxy adduct

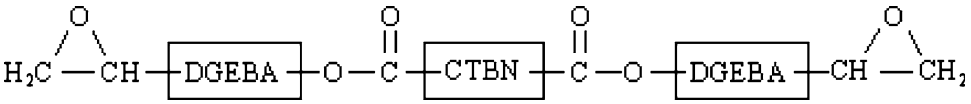


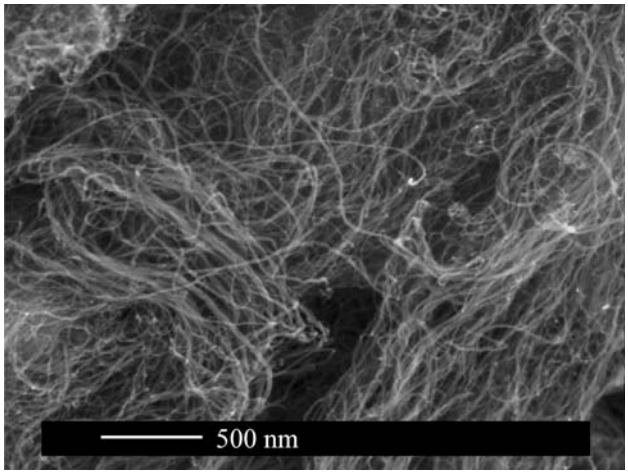


**Fig. 2** Scanning electron micrograph (FEG-SEM) of NC-7000 multi-walled carbon nanotubes, as supplied, showing a highly entangled structure

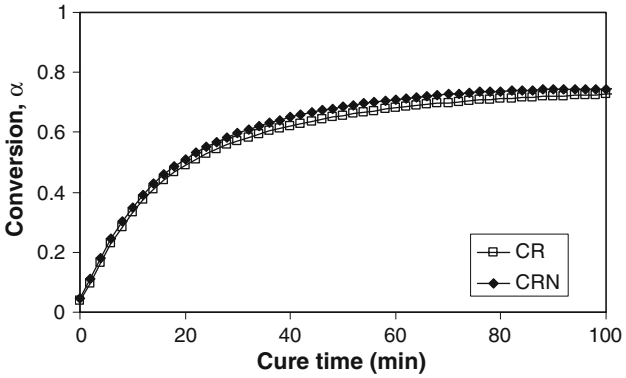


**Fig. 3** Conversion versus cure time at 120 °C, in the first 100 min. Conversion was determined by differential scanning calorimetry experiments, giving total reaction enthalpies as 449 and 380 J/g for CR and CRN formulations, respectively. Conversion was determined using a horizontal integration baseline, method described fully in [6]

As produced, the carbon nanotubes are highly entangled (Fig. 2), with a diameter in the region of 10 nm and length ranging from 0.1 to 10 μm. The mixture of carbon nanotubes and epoxy (without hardener) was stirred at 100 °C for 1 h at 3000 rpm using a high shear mixer (Dispermat CN10-F2); the mixture was then ultrasonicated, via a digital sonicator horn (Branson S-450D), operating at a frequency of 20 kHz, with maximum power setting of 400 W. The sonication energy input was determined by the need to hold the temperature at between 97 and 103 °C in order to maintain the relatively low viscosity [5]. The total specific energy input was 1.2 kJ/g.

The sonicated suspension was degassed, transferred back to the high shear mixer, mixed with the CTBN-epoxy adduct for 30 min at 3000 rpm and then with the hardener and the accelerator for another 30 min at 3000 rpm. During the stirring in of these constituents the mixture was kept under vacuum at 80 °C. Differential scanning calorimetry confirms that no significant cure reaction occurs in these systems at this temperature.

A shorthand nomenclature is used for identification of the samples. C is the abbreviation for the control formulation alone, CR for the control with rubber formulation, CN for the control with carbon nanotubes formulation and finally, CRN denotes the control formulation containing both rubber and carbon nanotubes.

Flat plaques of thicknesses between 3 and 6 mm were cast from all the formulations, in waxed glass moulds with metal inserts, after thorough degassing. They were cured in an air oven under partial vacuum. The curing cycle was 6 h at 120 °C for all the formulations, which was believed to be well in excess of the time required to achieve complete cure at this temperature—see Fig. 3.

## Conversion and glass transition temperature, $T_g$

The glass transition temperatures, determined by modulated differential scanning calorimetry (MDSC) measurements on cured samples, at a heating rate of 1 °C/min and with temperature modulation of 1 °C and period of 60 s, only varied between 133 and 134 °C for all the various formulations. Despite the prolonged cure at 120 °C, these samples were found to have reached final conversion levels of between only 73 and 75%. The rates of crosslinking in the early stages of cure in the base resin appeared unchanged by the presence of the nanotubes, which agrees with previous (unpublished) observations in our laboratory. However, all the blended samples exhibited great sensitivity to any increase in cure temperature above 120 °C, in that significant post-cure drifts in the glass transition temperature were observed in experiments carried out by dynamic mechanical analysis. The 120 °C cure does not drive the reaction to chemical completion, even after 6 h, in any of the formulations. Post-cure can thus be expected when the solid samples are heated above this temperature and to be more pronounced in the CNT-containing samples. Post-cure experiments were carried out to determine the ultimate achievable $T_g$ values in these systems and the results from MDSC measurements are shown in Table 1. To get stable values of $T_g$ it was necessary to post-cure the samples at 200 °C for 80 min; this is far above any

**Table 1** Compositions of the formulations employed and thermal analysis data, with ranges

| Sample | CTBN content (wt%) | MWCNTs content (wt%) | $T_g$ (°C) MDSC | CTE ($10^{-6}$ $K^{-1}$) | $T_g$ (°C) MDSC, after post-cure |
|---|---|---|---|---|---|
| C | 0 | 0 | 133 ± 1 | 51.93 ± 0.03 | 163 ± 1 |
| CR | 5 | 0 | 134 ± 1 | 52.11 ± 0.39 | 158 ± 1 |
| CN | 0 | 0.3 | 133 ± 1 | 51.84 ± 1.01 | 165 ± 1 |
| CRN | 5 | 0.3 | 134 ± 1 | 51.62 ± 0.77 | 162 ± 1 |

CTE values obtained from samples that were not post-cured

intended practical application of such blends but is probably an indication of the extent of diffusional limitations on the final stages of cure.

The fully cured samples exhibit a slight drop in $T_g$ consequent on the incorporation of the rubber—this is as expected in a phase separated system in which a very small proportion of the rubber remains dissolved within the continuous epoxy phase. Using the well-known Fox equation [7], the amount of rubber that has not phase separated and remains dissolved in the epoxy is estimated to be a very low proportion (~2%) of the total rubber added.

In contrast, the incorporation of the nanotubes results in a very slight increase in the final $T_g$ of the resin, as previously noted by other authors [8, 9]. The combination of the effects means that the final achievable $T_g$ in the CRN blend is indistinguishable from that achievable in the initial control resin.

### Coefficient of thermal expansion

The thermal expansion coefficients of cured specimens were measured using a thermal mechanical analyzer (TA Instruments 2940). Rectangular specimens of 5 × 5 × 10 mm were used (BS ISO 11359-2). After placing the specimen in the cell, the linear dimension of the sample was monitored from −50 °C to 100 °C at a heating rate of 1 °C/min. A slow cooling and reheating cycle was used in order to remove the effect of any initial residual stresses in the polymer and the thermal expansion coefficients were obtained from the second heating cycle, from the slope of the extension versus temperature curve in the temperature range of interest. The values at room temperature were determined from an average of three specimens and are shown in Table 1. The differences in the values for the specimens tested here cannot be considered significant, in the room temperature region or indeed any other region between −50 °C and 100 °C. In this respect, the inclusion of the nanotubes fails to deliver on the initial promise of property modification.

## Balance of mechanical properties

Flexural tests were performed using the three-point bending configuration at a crosshead speed of 1 mm/min according to the BS ISO178 test standard. The dimensions of the specimens were 3 × 15 × 80 mm for C and CR formulations and 2 × 12 × 60 mm for CN and CRN formulations. The span to thickness ratio *L*/*D* was set at 16 for all the formulations. The stress–strain dependence was linear and the flexural modulus $E_f$ was determined in the region between 5 and 25% flexural strain in the beam, as an average from five specimens, as shown in Table 2.

The compression yield stress, $\sigma_{yc}$ was obtained from uniaxial compression testing of six 3 × 5 × 6 mm specimens using a crosshead speed of 0.6 mm/min (BS ISO604), see Table 2. The compression test fixture used was a 10 kN rated Instron compression cage. This test jig is self aligning in that the movable crosshead moves downwards, compressing the specimen between two parallel plate faces as shown in Fig. 4a. No lubricating agent was used on the specimen surfaces and the experiments were stopped before any global buckling or barrelling had occurred. The stress–strain curves showed a clear yield point, taken as the maximum engineering stress. The post-

**Table 2** Mechanical properties of the cured samples, with standard deviations

| Sample | $K_{IC}$ (MPa $m^{0.5}$) | $E_f$ (GPa) | $\sigma_{yc}$ (MPa) |
|---|---|---|---|
| C | 0.8 ± 0.1 | 3.4 ± 0.1 | 141 ± 1 |
| CR | 1.1 ± 0.1 | 2.9 ± 0.1 | 114 ± 2 |
| CN | 0.9 ± 0.1 | 3.2 ± 0.1 | 141 ± 1 |
| CRN | 1.3 ± 0.1 | 2.7 ± 0.1 | 113 ± 2 |

Properties obtained from samples that were not post-cured

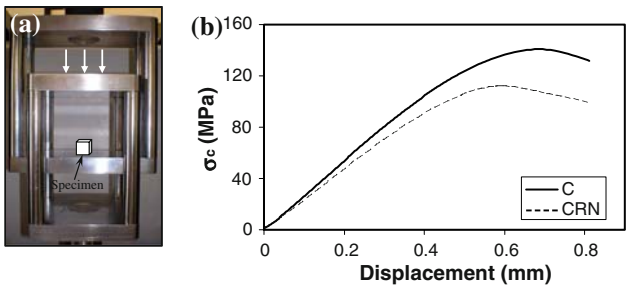


**Fig. 4** **a** Compression cage, with a schematic of specimen loading (not to scale). **b** Stress–displacement curves under compression loading, for C and CRN samples

yield strain softening observed in these samples (Fig. 4b) is recognised as an essential pre-requisite of a toughenable thermosetting system [10].

The fracture toughness ($K_{IC}$) and fracture energy ($G_{IC}$) were determined according to the BS ISO 13586 test standard. The values were taken from an average of five single edge-notched bending (SENB) specimens measuring 4 × 15 × 80 mm for the C and CR formulations and 3 × 12 × 60 mm for the CN and CRN formulations. The notch on the specimen edge was machined to a depth of at least 40% of the specimen width. Prior to testing, a sharper notch was introduced by tapping a pristine razor blade into the base of the machined notch. The new notch depth was between 45 and 55% of the specimen width. For all the formulations the specimens were tested in a three-point bend configuration using a span 4 times greater than the specimen width and a crosshead speed of 10 mm/min. Visual inspection of the fracture surfaces revealed no air bubbles; the C and CN specimens exhibited a mirror fracture surface whilst the fracture of the CR and CRN samples resulted in a slightly matt fracture surface but without any noticeable whitening. The fracture toughness results obtained are summarised in Table 2. The aromatic nature of the hardener limits the toughenability of the system, compared to more conventional rubber-toughened epoxies.

## Electrical properties of cured samples

Rectangular specimens of 4 × 12 × 30 mm were used to measure DC electrical resistivity. The cross-sectional areas were painted with silver paint to provide good contact. Electrodes were connected to the test specimens on both sides and two-terminal DC resistance measurements were performed using a 6517A Keithley electrometer, typically used for high resistance materials. The resistance of the formulations containing carbon nanotubes, CN and CRN, were obtained using a combination of a precision current source (6220 Keithley Instruments) and a nanovoltmeter (2182A Keithley Instruments) appropriate for lower measuring ranges. The values reported in Table 3 were taken after 1 min of voltage application, determined on five specimens. The AC electrical response of the materials was investigated using a Solartron SI 1260 frequency response analyser. Twenty-seven frequencies in the 1 Hz to 3.16 MHz range were swept on a logarithmic scale using an excitation voltage of 1 V. The conductivity, which was calculated as:

$$\sigma(f) = \frac{d}{|Z^*(f)|S}$$

where $d$ is the thickness, $S$ the area and $|Z^*(f)|$ the complex impedance, is illustrated as a function of frequency in Fig. 5. The base formulations follow a pure capacitive behaviour with the characteristic slope of unity in the conductivity versus frequency log–log plots. In contrast, the nanocomposites show a frequency independent conductivity, characteristic of ohmic behaviour. This behaviour, which is typically observed in nanotube–epoxy composites with nanotubes forming a conductive network [11], is maintained up to a certain inflection frequency over which a transition to a dielectric response occurs. The AC spectra can be used for the evaluation of the DC properties using the plateau conductivity observed at low frequencies for nanocomposites. The values obtained are identical to the DC measurements reported in Table 3.

**Table 3** Direct current electrical conductivities of the formulations in a solid state, with standard deviations

| Sample | $\sigma$ (S/m) |
|---|---|
| C | $<10^{-9}$ |
| CR | $3.2 \times 10^{-9} \pm 1.1 \times 10^{-9}$ |
| CN | $1.6 \times 10^{-3} \pm 2.3 \times 10^{-4}$ |
| CRN | $3.6 \times 10^{-3} \pm 3.2 \times 10^{-4}$ |

Properties obtained from samples that were not post-cured

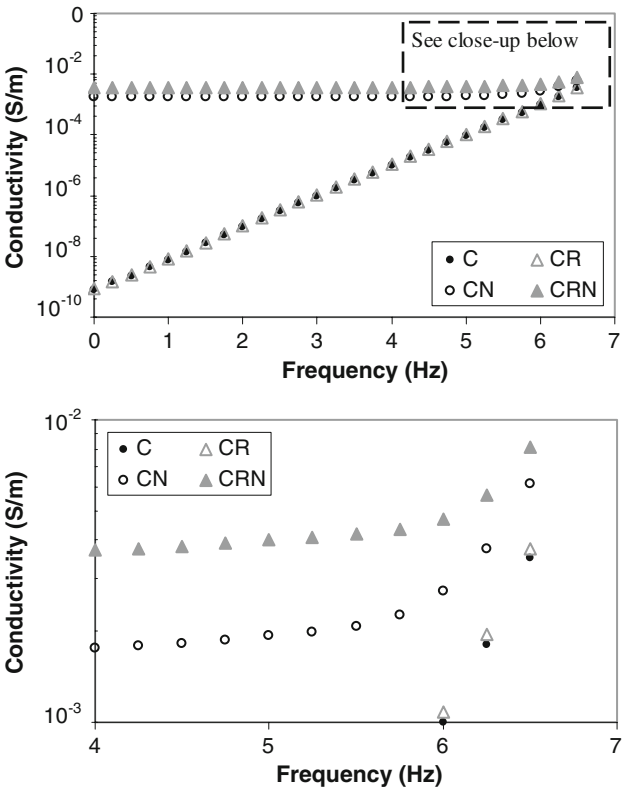


**Fig. 5** AC conductivity spectra for the base formulations and for the nanocomposites. The close-up graph at the *bottom* shows detail of the response of nanocomposites at the higher frequencies

## Structure–property relationships

Scanning electron microscopy (SEM) was used to examine cryo-fracture surfaces of the samples. The samples containing rubber were etched in toluene for 2.5 h at ambient temperature in order to extract the dispersed rubber phase [12].

Figure 6a, b shows SEM micrographs of the cryo-fracture surfaces of the formulations containing nanotubes; CN and CRN. In these images the bright dots are the ends of carbon nanotubes. Qualitative investigation of a large number of similar micrographs reveals the carbon nanotubes homogeneously dispersed, without any large agglomerates. The presence of the nanoparticles reflects itself in a significantly increased roughness of the fracture surface surrounding the CNTs, as previously noted by other authors [13].

All the formulations containing rubber displayed a two-phase morphology with an epoxy rigid continuous phase and a dispersed rubbery phase of isolated spherical particles. The nanotubes are believed to be associated with the epoxy phase, but presence of nanotubes within some rubbery particles cannot be discounted. On these micrographs only the imprints of the (cavitated and subsequently etched out) rubber particles are visible. The darker round holes indicate some porosity in the samples, but this is not significantly higher than might be expected in any cured epoxy sample.

The important information to be gained from Fig. 7a, b is the change in the distribution and sizes of the precipitated rubber particles for the CR and CRN formulations, respectively. Whilst difficult to quantify, the mean size of the rubber particles was demonstrably larger in the CR formulation than in the CRN sample. This decrease in size with the addition of the carbon nanotubes is thought to be associated with the increase in viscosity of the system caused by the dispersed nanotubes, which would inhibit the growth of the rubbery domains in the pre-gel phase [14]. The possibility of particle nucleation being enhanced by the nanotubes cannot be discounted, but has not been demonstrated.

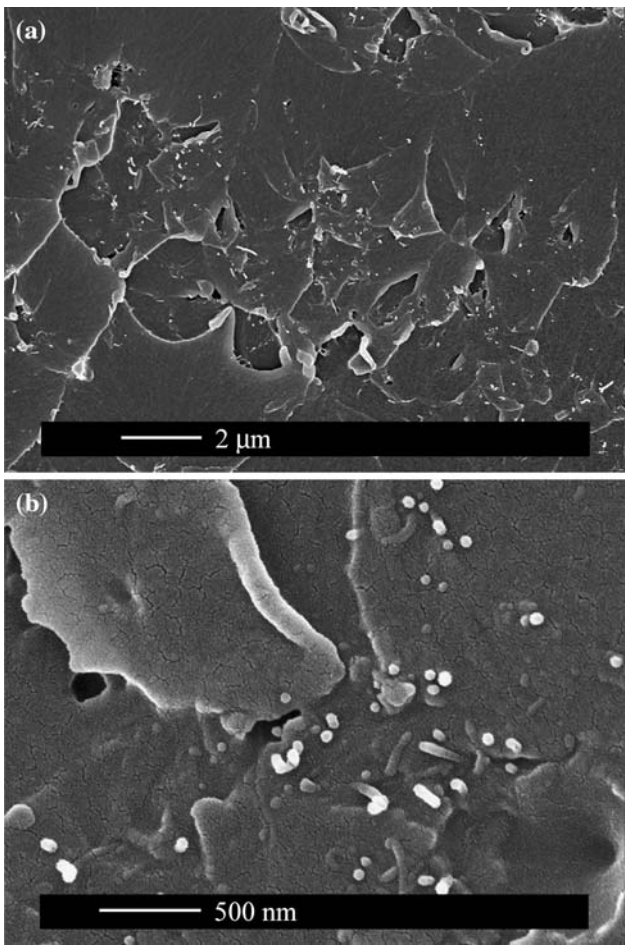


**Fig. 6** Scanning electron micrographs (FEG-SEM) of cryo-fracture surfaces for **a** CN and **b** etched CRN

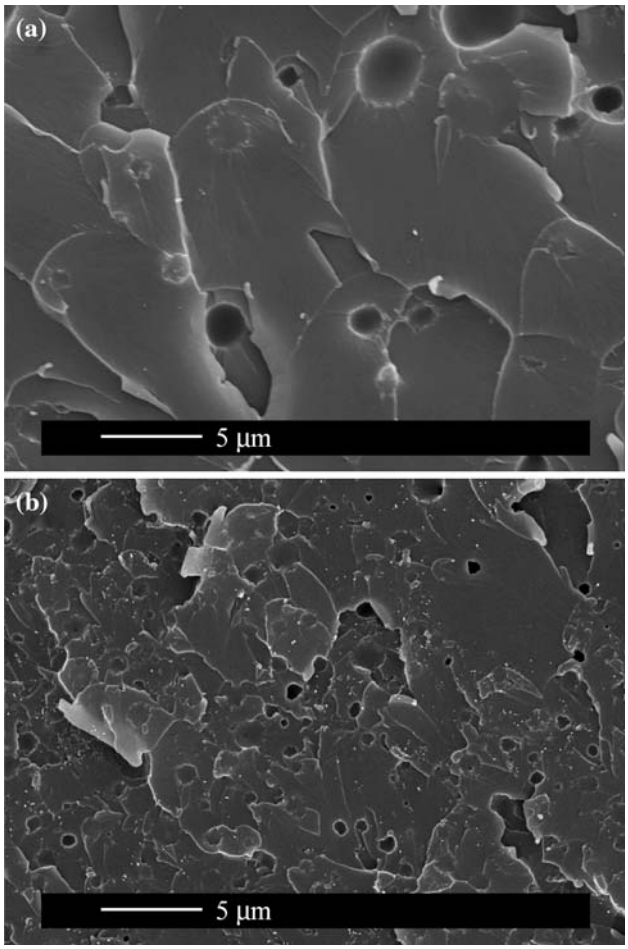


**Fig. 7** Scanning electron micrographs (FEG-SEM) of etched fracture surfaces for **a** CR and **b** CRN

It is thought that the high starting viscosity of the CRN mixture is beneficial in maintaining the quality of the CNT dispersion, by preventing the re-agglomeration during cure that is otherwise often observed in thermosetting nanocomposites [15, 16].

In terms of the mechanical performance (see Table 2), the addition of the relatively low modulus, rubber-rich particles to the base formulation results in a reduction in the flexural modulus of 15%. This is as expected in rubber-toughened epoxies [3, 17, 18], whereas no stiffening effect of nanotubes has been found [19]. The compressive yield strength is reduced by the addition of rubber, again as expected; inclusion of carbon nanotubes shows no effect.

In the notched fracture tests, there is a small, but measurable increase in the stress intensity factor upon the addition of rubber to the control formulation. The addition of nanotubes alone shows no significant effect. However, the inclusion of nanotubes and rubber in the formulation provides a further increase in $K_{IC}$, over 10% above the value obtained when rubber is used alone. This synergistic effect on toughening is seen more clearly in the data shown in Fig. 8. In this particular system, the increase in fracture energy is accompanied by an increase in the electrical conductivity, giving the solid CRN samples an attractive overall balance of properties.

Future aerospace applications may require electrically conductive, polymer-based composites for static discharge, electrical bonding, interference shielding, primary and secondary power and current return through the structure [20]. Good electrical bonding of a joint is needed to assist in controlling and dissipating the build-up of electrostatic charge. Commercial adhesives exist that have been filled with high amounts (up to 60 vol.%) of powdered silver, nickel or carbon black to achieve electrical conductivity. Unfortunately such additives make the adhesive weaker. The very high conductivity of carbon nanotubes makes them excellent candidates for the production of conductive epoxy adhesives, capable of dissipating electro-static charge build-up [21], and the present work shows that the required conductivity levels can be achieved without a compromise in the mechanical performance.

The most notable effect found in this study is the reduction of the mean rubber particle size in the rubber-toughened epoxy samples also containing carbon nanotubes. The only other ternary nanocomposites system studied in the context of adhesives preparation, an anhydride cured epoxy, uses silica nanoparticles with CTBN rubber and no effects on phase separation are reported [22]. However, it should be noted that the silica nanoparticles have little effect upon the viscosity of the system, unlike the carbon nanotubes used in this study. The toughening mechanism in the silica particle ternary system is debonding of the silica nanoparticles accompanied by cavitation within the epoxy matrix.

The smaller rubber particles in the present CRN formulation are still large enough to be capable of cavitating under the triaxial stress field at the crack tip [23, 24] and would therefore be expected to be contributing to toughening by initiating shear yielding in the surrounding matrix, which is the conventional mechanism of epoxy rubber toughening. In the absence of quantified morphology information, namely the volume fractions of small and large particles, it is not practical to use existing rubber cavitation theories [25] to estimate the expected toughening contributions in the different systems. There is no specific evidence that a high proportion of small rubber particles are generally beneficial to the toughness of a rubber-modified epoxy, but there have been reports of beneficial effects of a bimodal particle size distribution in such systems [26, 27]. It is therefore possible that the carbon nanotubes have a positive effect on the toughness of a ternary blend, not by the creation of any new toughening mechanisms, but by indirectly enhancing the overall contribution of the existing, highly efficient, toughening mechanisms.

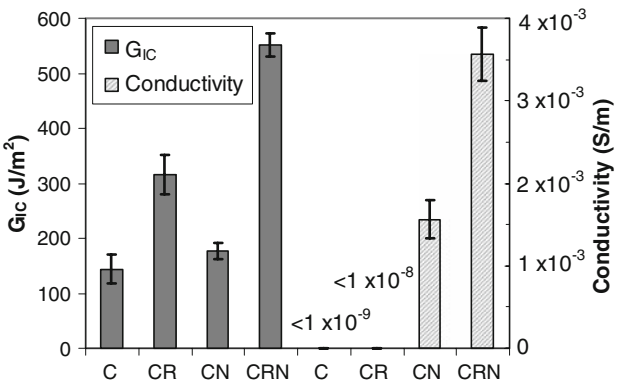


**Fig. 8** Fracture energy, $G_{IC}$, and electrical conductivity of the formulations employed

## Conclusions

The thermosetting ternary blends of epoxy, CTBN rubber and commercial carbon nanotubes, characterised in the present study, show that it is possible to achieve significant electrical conductivity at a low level of inclusion of CNTs and without a compromise in the thermo-mechanical performance of the adhesive. The good overall balance of properties is believed to be associated with the specific morphology of these systems, providing an efficient toughening mechanism as well as a conductive network.

**Acknowledgements** The work reported here was co-sponsored by EPSRC via a Speculative Research in Engineering award EP/C

509730 and by a Cranfield University IMRC project on 'Bonded Crack Retarders', supported by Airbus UK, Alcoa Inc. (USA) and Cytec Engineered Materials.

## References


1. Kwon YK, Berber S, Tomanek D (2004) Phys Rev Lett 92(1):1
2. Xu Y, Ray G, Abdel-Magid B (2006) Compos A 37(1):114
3. Verchère D, Sautereau H, Pascault JP, Moschiar SM, Riccardi CC, Williams RJJ (1989) Polymer 30(1):107
4. Kinloch AJ, Mohammed RD, Taylor AC, Eger C, Sprenger S, Egan D (2005) J Mater Sci 40(18):5083. doi:10.1007/s10853-005-1716-2
5. Battisti A, Skordos AA, Partridge IK (2009) Compos Sci Technol 69(10):1516
6. Skordos AA, Partridge IK (2001) Polym Eng Sci 41(5):793
7. Fox TG (1956) Bull Am Phys Soc 1(2):123
8. Gong X, Liu J, Baskaran S, Voise RD, Young JS (2000) Chem Mater 12(4):1049
9. Gojny FH, Schulte K (2004) Compos Sci Technol 64(15):2303
10. Huang Y, Hunston DL, Kinloch AJ, Riew CK (1993) In: Riew CK, Kinloch AJ (eds) Toughened plastics 1: science and engineering. Adv Chem Ser 233. Am Chem Soc, Washington, DC
11. Martin CA, Sandler JKW, Shaffer MSP, Schwarz MK, Bauhofer W, Schulte K, Windle AH (2004) Compos Sci Technol 64(15):2309
12. Thomas R, Durix S, Sinturel C, Omonov T, Goossens S, Groeninckx G, Moldenaers P, Thomas S (2007) Polymer 48(6):1695
13. Gojny FH, Wichmann MHG, Fiedler B, Schulte K (2005) Compos Sci Technol 65(15–16):2300
14. Williams RJJ, Rozenberg BA, Pascault JP (1997) Reaction-induced phase separation in modified thermosetting polymers. In: Koenis JL (ed) Adv Polym Sci, vol 128. Springer, Berlin
15. Fiedler B, Gojny FH, Wichmann MHG, Nolte CM, Schulte K (2006) Compos Sci Technol 66(16):3115
16. Sandler JKW, Kirk JE, Kinloch IA, Shaffer MSP, Windle AH (2003) Polymer 44(19):5893
17. Pearson RA, Yee AF (1986) J Mater Sci 21(7):2475. doi:10.1007/BF01114294
18. Kinloch AJ, Shaw SJ, Tod DA, Hunston DL (1983) Polymer 24:1341
19. Gojny FH, Wichmann MHG, Kopke U, Fiedler B, Schulte K (2004) Compos Sci Technol 64(15):2363
20. Baur J, Silverman E (2007) MRS Bull 32:328
21. Sandler J, Shaffer MSP, Prasse T, Bauhofer W, Schulte K, Windle AH (1999) Polymer 40(21):5967
22. Johnsen BB, Kinloch AJ, Mohammed RD, Taylor AC, Sprenger S (2007) Polymer 48(2):530
23. Dompas D, Groenickx G, Isogawa M, Hasegawa T, Kadokura M (1994) Polymer 35(22):4750
24. Liu J, Sue HJ, Thompson ZJ, Bates FS, Dettloff M, Jacob G, Vergese N, Pham H (2008) Macromolecules 41(20):7616
25. Bucknall CB, Paul DR (2009) Polymer 50(23):5539
26. Pearson RA, Yee AF (1991) J Mater Sci 26(14):3828. doi:10.1007/BF01184979
27. Partridge IK, Maistros GM (1995) Plast Rubber Compos Process Appl 23(5):325